Toward a fully autonomous hovercraft visually guided thanks to its own bio-inspired motion sensors

Frédéric Roubieu, Julien Serres, Stéphane Viollet, Franck Ruffier and Nicolas Franceschini

Institute of Movement Science - Biorobotics - CP938 - 163 av de Luminy
F-13288 Marseille, France

{frederic.roubieu, julien.serres, stephane.viollet, franck.ruffier, nicolas.franceschini}@univmed.fr

1. MOTIVATION, PROBLEM STATEMENT, RELATED WORK

Based on a biorobotic approach developed in our laboratory over the past 25 years, we have designed and built several terrestrial and aerial vehicles controlling their position and speed on the basis of optic flow cues (Franceschini et al. 1992, Viollet and Franceschini 1999, Ruffier and Franceschini 2005, Franceschini et al. 2007, Kerhuel et al. 2010).

In particular, in our project on the autonomous guidance of Micro-Air Vehicles (MAVs) in confined indoor and outdoor environments, we have developed a vision-based autopilot, which is called LORA III (Lateral Optic flow Regulation Autopilot, Mark III). This autopilot, based on the dual *optic flow regulation*, allows an air vehicle to travel along a corridor by automatically controlling both its speed and its clearance from the walls (Serres et al. 2008a). The *optic flow regulation* is a feedback control based on an optic flow sensor, which strives to maintain a perceived optic flow at a constant set-point by adjusting a thrust (Ruffier and Franceschini 2005).

The LORA III autopilot consists of a *dual optic flow regulator* in which each regulator has its own optic flow set-point and controls the robot's translation in one degree of freedom: a bilateral optic flow regulator controls the robot's forward speed, while a unilateral optic flow regulator controls the side thrust, making the robot avoid the walls of the corridor (Serres et al. 2008b). This autopilot draws on former studies which aimed to understand how a honeybee might be able to center along a corridor (Srinivasan et al. 1991), to follow a single wall (Serres et al., 2008b), and to adjust its speed according to the corridor width (Srinivasan et al. 1996).

Computer-simulated experiments have shown that a miniature hovercraft equipped with the LORA III autopilot can navigate along a straight or tapered corridor at a relatively high speed (up to 1m/s) (Serres et al. 2008a). The minimalistic visual system (comprised of only four pixels) may suffice for the hovercraft to be able to control both its clearance from the walls and its forward speed jointly, *without ever measuring speed or distance*, in a similar manner to what honeybees are thought to be capable of (Srinivasan et al. 1991, 1996, Serres et al. 2008b).

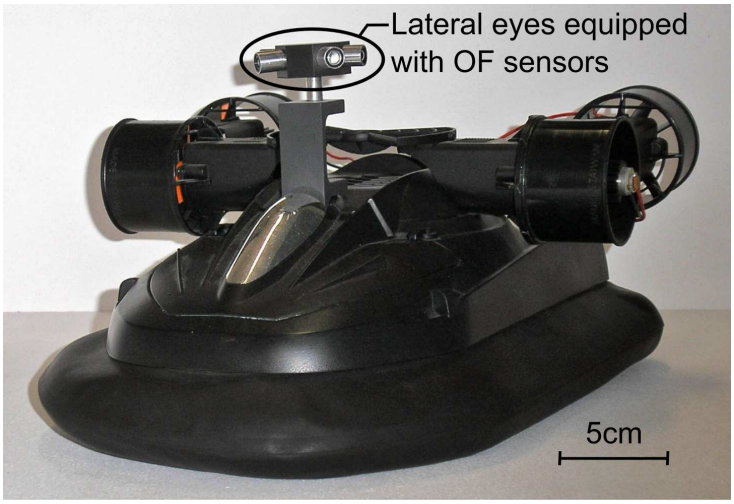

Figure 1. Sighted fully actuated hovercraft for testing the LORA III autopilot (Serres et al., 2008a).

The LORA robot (Fig. 1) is equipped with two rear thrusters and two lateral thrusters, in addition to the lift fan used to inflate the skirt. The hovercraft can move freely without any umbilicus, which makes its system identification and its own locomotion easier. However, the dynamics of all five motors turned out to be highly sensitive to the drop in supply voltage of the onboard Lithium Polymer (Li-Po) batteries. This is a critical issue for the identification of the robot's dynamical parameters. To perform an efficient system identification of the hovercraft's dynamics, we decided to confer upon each motor a dedicated controller that would make the four thrusters and the lift fan robust to any variations in the battery supply voltage.

2. HARDWARE INSIDE

The miniature hovercraft used here is a retrofitted version of a miniature RC hovercraft (Taiyo Toy LtD, Typhoon T-3, mass: 0.857kg, size: 0.36×0.21×0.17m). It makes no contact with the ground and it is endowed with inherent roll and pitch stabilization characteristics. Our hovercraft is fully actuated by two rear thrusters (surge axis) and two lateral thrusters (sway axis), and it can turn around its yaw axis by controlling differentially the rotational speed of the two rear thrusters. Two different Li-Po batteries provide the needed power and prevent low power electronics from being polluted by motor noise. The first one (7.2V, 2200mAh, size: 21×33×100mm, mass: 113g) is used for the motors, the second one (7.2V, 360mAh, size: 54×31×7mm, mass: 20g) is used for the low power electronics (compass, optic flow sensors…).

Each of the four thrusters is composed of a DC motor (7.2V, 24.5W, mass: 30g) loaded by a light three blades propeller (diameter: 4.9cm, mass: 0.8g) mounted onto the motor shaft. The brushless motor (Micro Rex 220/3-3200 Flyware, 7.2V, 37W, mass: 11g), controlled by an electronic speed controller (Hobbywing Pentium 10A, 9g, 17×27×6mm), is in charge of the hovercraft lift by rotating the lift fan (diameter: 7cm, mass: 19.6g).

For the speed regulation of the four thrusters, we used a four-ways 'sensorless' speed governor (regulator) (Viollet et al, 2008). This closed-loop speed regulator does not require any tachometers, which lightens the system and saves on energy. For the control of the brushless motor, we measured the lift fan rotational speed with a tiny infrared sensor (Fig. 2B) and regulated it with a speed controller based on a closed-loop control scheme (Proportional-Integrator controller).

The hovercraft perceives the visual environment by means of bio-inspired motion sensors also called Elementary Motion Detectors (EMD) (Ruffier et al. 2003, Ruffier Franceschini 2005, Pudas et al. 2007), which requires to only measure the translational optic flow. Any yaw disturbance is liable to introduce a rotational optic flow component, which is compensated for by a custom-made heading lock system composed of a micro-compass (HMC6052, precision: 0.3°, size: 24×18mm, mass: 2g) and a micro-gyrometer (ADXRS300, range speed: ±300°/s, size: 7×7×3mm, mass: 0.5g) implemented in an internal loop that controls the two rears thrusters differentially. The four visual motion sensors that compose the vision system are linked to the motor board through a galvanic isolation to preserve the signals from the motor noise.

A 'Bluetooth' module (F2M03GLA, size: 28.5×15.2×2mm) enabling wireless communication and monitoring was also implemented to improve the autonomy of the robot.

The size of the electronic motor board was reduced to a minimum (65×80mm) by using a double layer PCB design and a new generation microcontroller (dsPIC from Microchip©). Two different dsPICs are actually used: the first one (dsPIC33FJ128MC804, clock: 40Mhz, size: 8×8mm) is used to control the wireless module (Fig. 2A), the four thrusters and to read the four EMDs, the second one (dsPIC30F2010, clock: 20Mhz, size: 6×6mm) is used to control the brushless motor which actuates the lift fan.

During the implementation process, we used a custom-made "rapid control prototyping toolbox for dsPIC" to make easier the embedding (Embedded Target for Microchip dsPIC toolbox, http://www.kerhuel.eu/wiki/Simulink_-_Embedded_Target_for_PIC). This toolbox is efficient to program the Microchip's microcontroller directly from the Mathworks© environment (Simulink and Real-Time Workshop toolbox), without typing any C code lines.

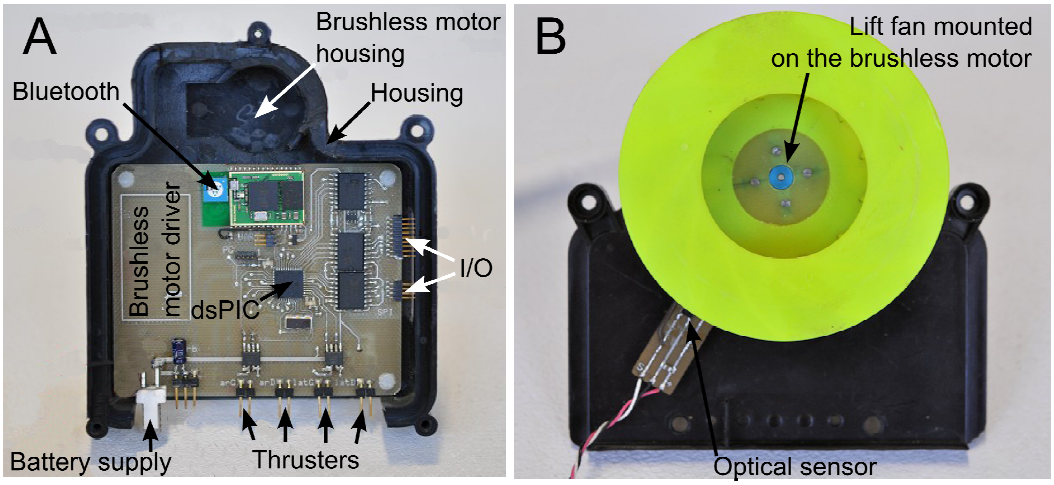

Figure 2. (A) Top view of the motor board in his housing. (B) The yellow lift fan is mounted on a brushless motor whose rotational speed is monitored by an infrared optical sensor.

3. RESULTS AND EXPERIMENTS

We tested here the responses of two speed control systems with respect to voltage supply disturbances:

1. the thrusters' speed governor,
2. and, the speed control of the lift fan mounted on a brushless motor.

The thrusters' speed governor

Figure 3 shows experimental results to fast supply voltage perturbations (from 8.4V to 5.9V on Fig. 3A and Fig. 3C) when the governor mode is off (Fig. 3A-B) and when the governor mode is on (Fig. 3C-D). The 'sensorless' speed governor provides the standard deviation of the propeller speed to be 10-fold reduced (from 13rps on Fig. 3B to 1.3rps on Fig. 3D).

The aeromechanical rise time of the propeller is 48ms in open loop and 45ms in closed loop (data not shown). The 'sensorless' speed governor therefore preserves the short rise time.

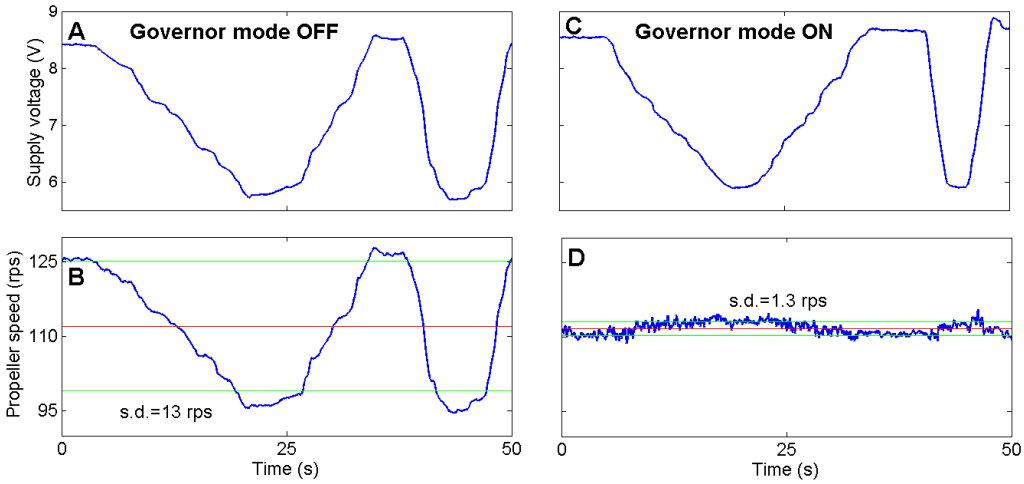

Figure 3. (A) & (C) The supply voltage, provided by a DC power supply (ELC, AL781NX), was changed manually. (B) When the governor mode is off, the propeller speed is strongly disturbed by the supply voltage variations. (D) When the governor mode is on, the propeller speed seems to be quasi-constant.

The speed control of the lift fan mounted on a brushless motor

Figure 4 shows experimental results to fast supply voltage perturbations (from 8V to 5.9V on Fig. 4A and Fig. 4C) when the speed controller is off (Fig. 4A-B) and when the speed controller is on (Fig. 4C-D). The speed controller provides the standard deviation of the lift fan speed to be about 10-fold reduced (from

13rps on Fig. 4B to 1.4rps on Fig. 4D). The speed controller of the lift fan mounted on the brushless motor compensates efficiently for variations of the supply voltage.

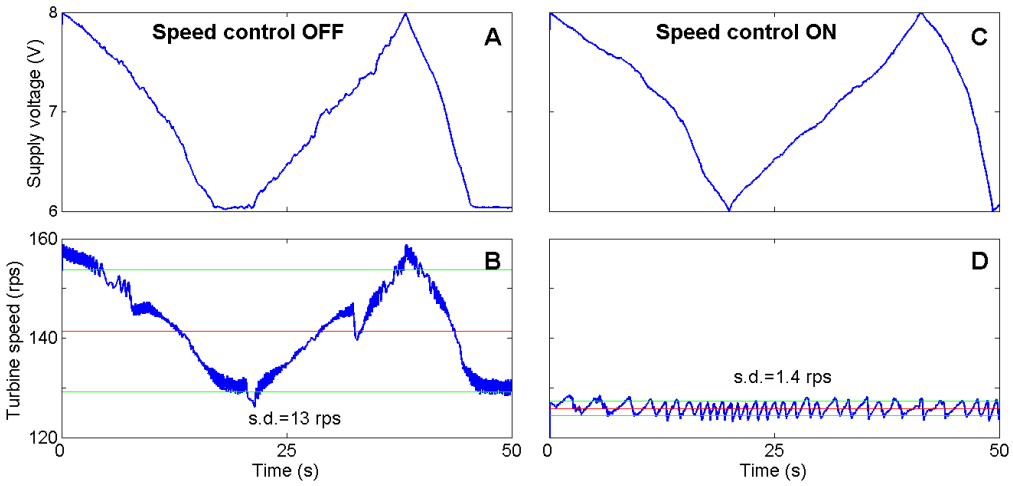

Figure 4. (A) & (C) The supply voltage, provided by a DC power supply (ELC, AL781NX), was changed manually. (B) When the speed controller is off, the lift fan speed is strongly affected by the supply voltage variations. (D) When the speed controller is on, the lift fan speed is quasi-constant.

4. MAIN EXPERIMENTAL INSIGHTS

The LORA III autopilot, inspired by motion vision in flying insects is a first step toward a deft, lightweight and power-lean visuo-motor control system for MAVs. The LORA III autopilot is meant to be embedded onboard a miniature seeing hovercraft (0.857kg) equipped with four elementary eyes (each made of only 2 pixels). This robot is fully actuated by four thrusters and a brushless motor actuates the lift fan for sustaining the hovercraft. One major issue is that by definition, the rotor speed of a motor is sensitive to variations of the supply voltage. We therefore developed two electronic boards making the rotor speed of the motors insensitive to any drops in the supply voltage. The first electronic board controls the DC motors of each of the four thrusters on the basis of a 'sensorless' speed governor (Viollet et al. 2008). This 'sensorless' regulator allows the rotor speed to be stabilized against large voltage disturbances (Fig. 3) and preserves the short rise time. The second electronic board allows the rotational speed of the lift fan to be stabilized by means of an optical sensor. The lift fan speed can be efficiently controlled and is robust to large voltage disturbances (Fig. 4).

Making the robot largely insensitive to voltage disturbances was a prerequisite for our current system identification, which will allow us to tune the controllers to the appropriate dynamic parameters of the LORA robot and to validate further our bio-inspired optic flow-based autopilot (Serres et al. 2008a).

5. REFERENCES

Franceschini, N., Pichon, J.M., & Blanes, C. (1992). From insect vision to robot vision. Philosophical Transaction of the Royal Society London B: Biological Sciences, 337:283-294.

Franceschini, N., Ruffier, F., & Serres, J. (2007). A Bio-Inspired Flying Robot Sheds Light on Insect Piloting Abilities. Current Biology, 17:329-335.

Kerhuel, L., Viollet, S., & Franceschini, N. (2010). Steering by gazing: an efficient biomimetic control strategy for visually guided micro aerial vehicles. IEEE Transactions on Robotics, 26(2): 307-318.

Pudas, M., Kruusing, A., Leppavuori, S., Boyron, M., Amic, S., Viollet, S., and Franceschini, N. (2007). A miniature bio-inspired optic flow sensor based on low temperature co-fired ceramics (LTCC) technology. Sensors and actuators A: Physical, 133:88-95.

Ruffier, F. & Franceschini, N. (2005). Optic flow regulation: the key to aircraft automatic guidance. Robotics and Autonomous Systems, 50(4):177-194.

Ruffier, F., Viollet, S., Amic, S., and Franceschini, N. (2003). Bio-inspired optical flow circuits for the visual guidance of micro-air vehicles. Proceeding of IEEE International Symposium on Circuits and Systems (ISCAS), 3:846-849.

Serres, J., Dray, D., Ruffier, F., & Franceschini, N. (2008a). A vision-based autopilot for a miniature air vehicle : joint speed control and lateral obstacle avoidance. Autonomous Robots, 25:103-122

Serres, J., Masson, G., Ruffier, F., & Franceschini, N. (2008b). A bee in the corridor: centering and wall following. Naturwissenschaften, 95(12) : 1181-1187.

Srinivasan, M.V., Lehrer, M., Kirchner, W.H., & Zhang S.W. (1991) Range perception through apparent image speed in freely-flying honeybees. Visual Neuroscience, 6:519-535.

Srinivasan, M.V., Zhang, S.W., Lehrer, M., & Collett T.S. 1996. Honeybee navigation en route to the goal: visual flight control and odometry. Journal of Experimental Biology, 199:237-244.

Viollet S., & Franceschini, N. (1999). Visual servo system based on a biologically-inspired scanning sensor. In proceeding of SPIE conf. on sensor fusion and decentralized control on robotics II (Vol. 3839, pp. 144-155), Boston, USA.

Viollet, S.V., Kerhuel, L. and Franceschini, N. (2008). A 1-gram dual sensorless speed governor for micro-air vehicles. Proc. IEEE 16th Medit. Conf. on Control & Automation (MED'08), 1270-1275.